INSTRUMENTATION FOR THE ASTA PHOTOCATHODE GUN AT SLAC

J. Corbett[†], S. Gilevich, E. Jongewaard, J. Lewandowski, J. Sheppard, P. Stefan, T. Vecchione, S. Weathersby and F. Zhou

SLAC National Accelerator Laboratory, Menlo Park, CA, 94025, USA

Abstract

An accelerator test stand has been constructed at SLAC to characterize laser-assisted photocathode processing, electron beam emission physics and front-end RF gun performance. The objective of the research program is to identify definitive 'recipes' for high-reliability photocathode preparation resulting in persistent high quantum efficiency and low beam emittance. In this paper we report on timing, optics and instrumentation for the Ti:Sapphire drive laser and diagnostics for the electron beam.

INTRODUCTION

The ASTA photocathode research program at SLAC features a frequency-tripled Ti:Sapphire laser targeting the backup RF gun for the LCLS injector [1,2]. The near-term goals are to develop reliable and repeatable methods for laser-assisted cathode processing leading to high quantum efficiency, low emittance and long cathode lifetime [3,4]. For optimal quantum efficiency (QE) it is desirable to illuminate the copper cathode with short wavelength UV light. Tests include replicating controlled and uncontrolled cavity venting, cathode swaps, laser processing under a range of fluence conditions and systematic QE mapping of the cathode surface over the course of time. Also of interest are QE dependence on cathode reflectivity and surface roughness, the effect of vacuum gas composition, dependence on laser beam intensity profile [5] and alternative cathode surfaces.

Functionally the laboratory closely resembles the LCLS injector [6] including laser hall, photon beam transport optics, PAC/PAD timing systems, RF power delivery and a subset of electron beam diagnostics. The laboratory layout consists of three adjacent rooms - a conventional control room running EPICS on linux computers, a Class 4 laser room containing the Ti:Sapphire laser, and a concrete bunker housing the electron gun. The RF modulator and klystron reside in a separate part of the building. This paper reports on technical aspects of the overall RF photocathode system with an emphasis on diagnostics and instrumentation.

DRIVE LASER

The Ti:Sapphire laser laboratory has been documented in reference [7]. Of note the laser system serves two independent research programs – the ASTA photocathode program (2ps UV pulses at 120Hz) and development of ultrafast timing diagnostics for the LCLS (25fs IR pulses at 1kHz). The basic laser components include a 68MHz Coherent Vitara oscillator operating at 760nm center

---

[†]corbett@slac.stanford.edu

frequency and a Legend Elite regen amplifier with dual stretcher/compressor optics for ps and fs operation, respectively.

To achieve laser/RF timing synchronization, the oscillator cavity is frequency locked at 476MHz to the 119MHz LCLS timing fiducial [8] via a Coherent SynchroLockAP® chassis. An internal photodiode connected a synchronized/delay generator (SDG) communicates the 68MHZ pulse arrival time to the regen. A second, external photodiode triggers SLAC-built PAC/PAD timing modules which provide a synchronous 120Hz clock to the regen for the pump laser and Pockels cells. The RF system is independently locked to the 119MHz LCLS timing fiducial via a second set of PAC/PAD modules using gun cavity field probes and forward RF power as input. The net effect of the parallel PAC/PAD timing systems is to synchronize the UV laser pulse to the RF drive at the photocathode gun.

UV Beam Conditioning

As illustrated in Fig. 1, the 68MHz oscillator seed beam first passes through a Pockels cell/thin film polarizer (TFP) combination to extract time-synchronous IR pulses for cross-correlator pulse length measurements. The seed
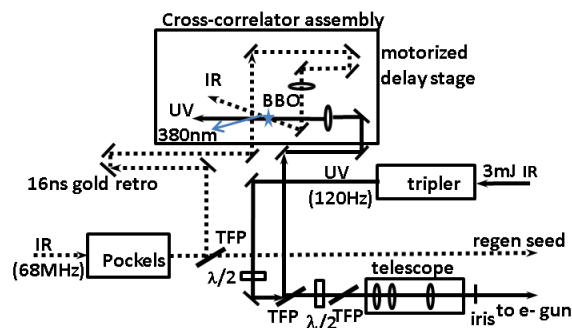

Figure 1: UV beam conditioning optics.

beam is then stretched, amplified and compressed (CPA) in the regen. Upon exit from the regen, the compressed IR beam enters a frequency tripler to generate ~300μJ UV pulses at 253nm. Dichroic mirrors isolate the 253nm component and a half-waveplate/TFP combination extracts a fraction of each UV pulse for the cross-correlator. A second HWP/TFP with an EPICS controlled Newport rotation stage adjusts UV power at the cathode.

The UV transport line begins with a three-lens telescope consisting of a beam expander/collimating lens combination mounted on a sliding rail to illuminate the primary iris. By varying the iris diameter and/or UV beam

size the impact of laser intensity profile on beam emittance can be studied [5]. The iris plane is imaged via relay optics onto the photocathode surface with a 4.5:1 beam size reduction ratio and 33% power transmission. Three evacuated transport tubes equipped with DUV grade fused-silica viewport windows route the UV beam onto a 50cm x 100cm optical bench adjacent to the electron gun.

As illustrated in Fig. 2, a fraction of the UV beam is sent to a Coherent PowerMax® joule meter to monitor pulse energy. The ratio of laser energy at the joule meter to laser energy at the cathode is 1:9. A motor-controlled steering mirror (M2) positions the photon beam at the photocathode. The steering system is used to center the electron beam in the magnetic solenoid, raster the laser during cathode processing and for QE surface scans.

A beam splitter downstream of M2 deflects a fraction of the beam to the UV-sensitive 'virtual cathode camera' (VCC) positioned at the same path length as the gun cathode surface. Also shown in Fig. 2 is an insertable focusing lens used for cathode surface processing. With the lens inserted, a 3.5μJ UV pulse into a 30um spot size generates an energy density of ~1mJ/μm^2. During a typical processing scan the laser dwell time is 30 shots/spot. The motorized HWP/polarizer combination in
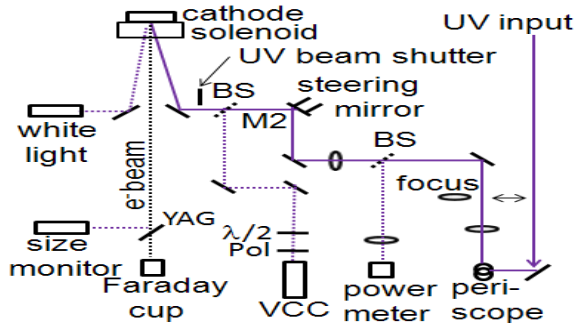

Figure 2: Schematic diagram of beam diagnostic system at the photocathode gun location.

front of the VCC is used to protect the CCD camera during laser processing.

UV/IR Cross-Correlator

A scanning cross-correlator (CC) was constructed to measure the UV pulse duration. The CC mixes a fraction of the UV beam power with 25fs pulses from the IR oscillator in a Type-II BBO crystal. As shown in Fig. 3, the UV and IR pulses are routed to a 30cm x 30cm optical breadboard containing the BBO. To optimize the overlap signal both beams are focused just beyond the BBO medium. Coarse timing between the UV and IR beams is adjusted with a gold mirror retro-reflector delay line mounted on a 1 m rail. The vernier delay stage shown to the lower left in Fig. 3 is controlled by a Newport motor under EPICS control.
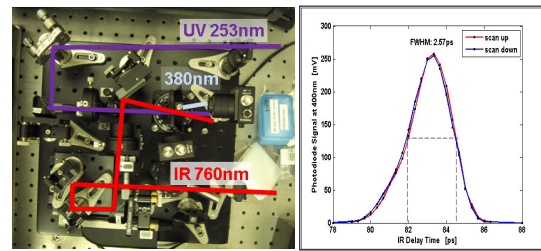
Figure 3: (a) Plan view image of UV/IR cross- correlator and (b) typical cross-correlation scan.

Spatio-temporal overlap is achieved by first centering the two beams in a 100μm diameter pinhole centered at the BBO crystal plane and then monitoring diffuse scattering of the UV and IR pulses with a fast photodiode to achieve synchronization at the few hundred ps level. The cross-correlation signal is then found by careful rotation of the BBO about the vertical axis and fine tuning time synchronization with the vernier delay stage. Conservation of photon momentum places the 380nm blue beam exiting the BBO to the left of the 253nm UV beam as shown. A limiting iris and 380nm bandpass filter isolate the blue beam entering the photodiode. The output signal is read into the same analog signal digitizer used to

Figure 4: LCLS photocathode gun with solenoid, water feeds and RF waveguide.

measure beam charge at the Faraday cup (see below). A typical cross-correlation scan for a 2.5ps rms pulse is shown in Fig. 3(b).

PHOTOCATHODE GUN

The LCLS electron gun design features a 120Hz, 1.6-cell cavity design with dual-feed RF coupling to minimize the dipole field component [9]. The high-purity copper cathode material was chosen in part to permit the entire end plate of the half cell to be formed from a single piece, allowing gun operation at the highest possible field values. The complete gun assembly includes a solenoid, bucking coil, vacuum pumps, and steering magnets. Diagnostics include cavity probes, waveguide directional couplers, a cold cathode vacuum gauge, RGA, thermocouples and RTDs. Typical cavity pressures are ~1.3nT under at full RF power. The RGA provides an in-situ diagnostic to monitor gas components for different environments, such as RF/laser on/off and laser cleaning on/off.

Following a sequence of hydrogen furnace braze, diamond flycut and vacuum firing, a typical LCLS cathode yields an initial QE ranging from low 10^{-6} to mid
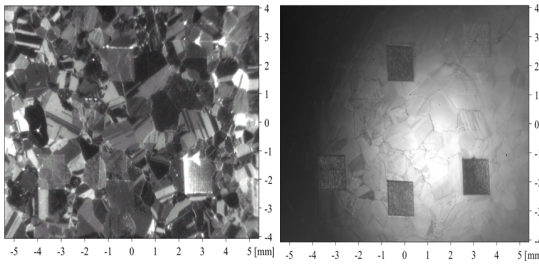
Figure 5: High-resolution photocathode images with 90° incident light (left) and 30° incident light showing laser processed areas and grain boundaries.

10^{-5} after RF cavity processing. For LCLS operations, QE values $>2x10^{-5}$ are needed to produce a few 100pC beam charge with ~10 μJ UV pulse energy.

To date laser-assisted cathode surface processing has proven to be the most effective means to achieve the desired QE.

Cathode Imaging System

In the course of processing the photocathode surface it is important to understand the physical impact of the laser beam on the cathode surface. For this purpose a conventional 1600x1200 pixel GigE CCD camera is configured to view the cathode via a second in-vacuum mirror adjacent to the primary UV beam input mirror. The photocathode camera is mounted at a working distance of 527 mm. It uses a 235 mm focal length lens NIKKOR zoom lens (Nikon AF-S DX 55-300mm f/4.5-5.6G ED VR) with a 190 mm extension tube composed of a 150 mm variable Zykkor Macro Bellows and CCTV lens tubes to give an overall magnification of 0.807.

Ambient lighting can be either normal to the photocathode surface or incident at 30 degrees depending on the desired image contrast. Images are acquired within a few seconds exposure time. Due to aperture restrictions the system has a diffraction limited spatial resolution of a few tens of microns. Imaging is fine-focused by minimizing the size of image features while varying the working distance.

Figure 5 shows high-resolution images of the photocathode surface after laser processing. The images were obtained with 90° and 30° white-light illumination from a fiberoptic lamp. Each composite picture was made by stitching together individual images in software. Although the data are indicative of surface reflectivity, behavior in the UV is expected to vary. Further magnification of laser processed areas clearly shows the physical 'crater' impact of the laser beam at each processed point.

ELECTRON BEAM DIAGNOSTICS

The electron beam line is equipped with vacuum pumps, diagnostics, and isolation valves to facilitate cathode swaps, gun changes and future modifications. The e⁻ beam is focused by a magnetic solenoid onto a

Faraday cup located 1.4 m downstream of the cathode. Corrector dipole magnets provide beam position and steering control. A beam position monitor has been installed in front of the Faraday cup but signal processing electronics have not yet been connected.

Beam Energy

The beam energy is calculated using the measured X-Y rotation due to the solenoid. For this measurement, the laser steering mirror M2 is swept in one plane (X) and the horizontal and vertical motion on the profile monitor is noted, dX/d(M2) and dY/d(M2). The rotation angle is given by

$$\varphi_{rot} = \operatorname{atan}\left(\frac{\frac{dx}{d(M2)}}{\frac{dy}{d(M2)}}\right) = BL/2$$

with *BL* the integrated solenoid strength (kG-m) [10]. For 10MW forward power into the gun and the rf phase set to
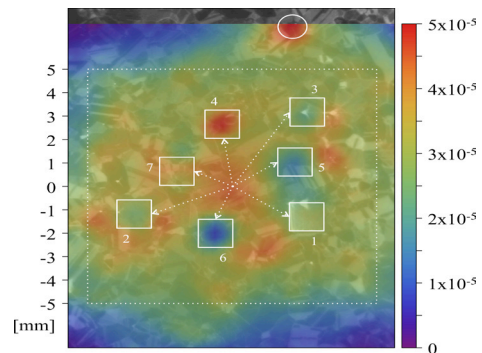

Figure 6: Quantum efficiency map across photocathode with 7 laser-processed spots indicated.

-30°, the beam energy was measured to be 5.5±0.05MeV. The error on the measurement is taken as the standard deviation of 3 data points taken at 3 different solenoid settings.

Faraday Cup

An LCLS style Faraday cup is used to measure the charge out of the gun. The charge collection efficiency of the Faraday cup is estimated to be 78% [11]. Charge collected in the cup is feed into an LMR-241 cable and monitored using a CAEN V965 QDC and a Textronic TDS3054B oscilloscope. Both the QDC and scope signals are read into the ASTA EPICs control system. The dynamic range for the QDC system varies from about 40pC to 1 nC; the dynamic range for the scope system varies from about 0.5pC-2nC. Figure 6 shows an example of a QE surface map measured by scanning the UV beam across the photocathode.

Beam Profile and Emittance Diagnostic

The ASTA profile monitor consists of a 50 mm diameter, 100 micron thick Ce:YAG screen and an AVT

Prosilica GE 1660 camera with 5.5 micron pixel size. The YAG screen camera is mounted at a working distance of 293 mm. It uses a 87 mm focal length SIGMA zoom lens (Lambda II Nikon F 75-300mm f/4.5-5.6) with a 37 mm extension tube, giving a magnification of 0.424. Images of the YAG screen are nominally acquired in 0.1-0.2 seconds. The imaging system has a pixel limited spatial resolution of 13 microns. Full system resolution (screen, lens, camera) is estimated to be ~35μm, rms.

Emittance measurements are made using the Ce:YAG screen in conjunction with the gun solenoid. A Matlab GUI application which has been copied over from the LCLS is used to control the machine and process the raw data. This application has the ASTA-LCLS beamline geometry hard-coded into the calculation. An addressable MatlabPV allows the user to enter the beam energy; a thick lens model of the solenoid is used and the computed beam energy is referenced to the entrance of the solenoid. Space charge is not included in the calculation and rotation through the solenoid is ignored, i.e. it is assumed that the beam is round. Because of space charge, beam emittance has been typically measured for bunch charges of 1-2pC with the Schottky phase -15 degrees. For solenoid scan emittance measurements, the minimum beam size is ~100 microns. For beams at the center of the cathode, $\gamma\varepsilon_x=\gamma\varepsilon_y=0.30\pm0.01$ m-rad for a 250μm rms incident laser spot size.

SUMMARY

The LCLS electron gun is presently operating with a third photocathode. Experience has shown the initial QE can be well below the few 10^{-5} target value without laser cathode processing and that the evolution of QE can be a complicated function of time. The ASTA program provides a facility to systematically investigate cathode physics under a variety of controlled laser, RF and vacuum conditions. Significant diagnostics at ASTA include laser power meters, the VCC, a white-light cathode imaging camera, Ce:YAG scintillation screen, Faraday cup and emittance measurement via solenoid field scan. Instrumentation not described in this paper include timing jitter measurements and RF power diagnostics.

In the near term the ASTA program will continue to carry out detailed photocathode characterization and test fs e-beam pulse production using a CsBr-coated copper cathode. Future plans call for the addition of an energy-resolving spectrometer and installation of quadrupoles with a pepperpot screen for emittance measurements while leaving the gun solenoid at fixed field.

REFERENCES

[1] E. Jongewaard, et al, "RF Gun Photocathode Research at SLAC", IPAC12, New Orleans (2012).

[2] T. Vecchione, et al, "SLAC RF Gun Photocathode Test facility", FEL2013, New York (2013).

[3] D. Dowell and J. Schmerge, "Quantum Efficiency and Thermal Emittance of Metal Photocathodes", PRSTAB 12, 074201 (2009).

[4] F. Zhou, et al, "High-Brightness Electron Beam Evolution following Laser-Based Cleaning of a Photocathode", PRSTAB 15, 090703 (2012).

[5] F. Zhou, et al, "Impact of the Spatial Laser Distribution on Photocathode Gun Operation", PRSTAB 15, 090701(2012).

[6] R. Akre, et al, "Commissioning Results of the LCLS Injector", FEL2007, Novosibirsk, Russia (2007).

[7] J. Corbett, et al, "Short-Pulse Laser for Photocathode Research at SLAC", IPAC13, Shanghai, China (2013).

[8] P. Krejcik, et al, "Timing and Synchronization at the LCLS", DIPAC07, Venice, Italy (2007).

[9] D.H. Dowell, et al, "The Development of the Linac Coherent Light Source RF gun", ICFA Beam Dynamics Newsletter 46 (2008) 162-192.

[10] R. H. Helm, "Adiabatic Approximation for Dynamics of a Particle in the Field of a Tapered Solenoid", SLAC-Report-04, August, 1962.

[11] M. Leitner, "Charge Collection Efficiency Studies for LCLS and LCLS-II Faraday Cups", SLAC Radiation Physics Note RP-11-09, October 21, 2011.